Temperature sensing of adipose tissue heating with the luminescent upconversion nanoparticles as nanothermometer: In vitro study

I.Yu. Yanina,[*1,2] E.K. Volkova,[1,2] A.M. Zaharevich,[1] J.G. Konyukhova,[1]
V.I. Kochubey,[1,2] V. V. Tuchin[1,2,3]
[1]Saratov National Research State University, Russian Federation
[2]National Research Tomsk State University, Russian Federation
[3]Institute of Precision Mechanics and Control RAS, Russian Federation

[*]e-mail: irina-yanina@list.ru

Abstract

The luminescence spectra of upconversion nanoparticles (UCNPs) imbedded in fat tissue were measured in a wide temperature range, from room to human body and further to hyperthermic temperatures. The two types of synthesized UCNP [$NaYF_4$:Yb^{3+}, Er^{3+}] specimens, namely, powdered as-is and embedded into polymer film, were used. The results show that the luminescence of UCNPs placed under the adipose tissue layer is reasonably good sensitive to temperature change and reflects phase transitions of lipids in tissue cells. The most likely, multiple phase transitions are associated with the different components of fat cells such as phospholipids of cell membrane and lipids of fat droplets. In the course of fat cell heating, lipids of fat droplet first transit from a crystalline form to a liquid crystal form and then to a liquid form, which is characterized by much less scattering. The phase transitions of lipids were observed as the changes of the slope of the temperature dependence of UCNP luminescence intensity. The obtained results confirm a high sensitivity of the luminescent UCNPs to the temperature variations within tissues and show a strong potential for providing a controllable tissue thermolysis.

Keyword list: upconversion nanoparticles, adipose tissue, phase transition, nanothermometer

1. INTRODUCTION

Luminescence-based techniques are excellent tools to investigate fundamental processes in life sciences. They represent extremely important and powerful (bio)-analytical approaches in medicine, biology, and chemistry due to their fast, sensitive (down to the single-molecule level), reliable, and reproducible detection procedures. There is a large variety of molecular chromophores (e.g. organic dyes, metal-ligand complexes, lanthanide chelates, or fluorescent proteins) from which one can choose for (bio)-imaging and sensing applications.[1]

Almost all luminescent nanomaterials require excitation by UV or visible light and show Stokes-shifted emission (i.e. the emitted light has a longer wavelength than the excitation light. Therefore, they can be designated as downconverting luminescent nanomaterials (nanoparticles). However, in recent years, a new class of nanoscale luminophores, which are referred to as upconverting luminescent nanoparticles, has gained much scientific interest. Here, the emitted light has a shorter wavelength than the excitation light.[2] Upconversion (UC) utilizes sequential absorption of multiple photons through the use of long lifetime and real ladder-like energy levels of trivalent lanthanide ions embedded in an appropriate inorganic host lattice to produce higher energy anti-Stokes luminescence.[2,3] It thereby converts two or more low-energy excitation photons, which are generally NIR light, into shorter wavelength emissions (e.g., NIR, visible, and UV). This process is different from nonlinear multiphoton absorption in organic dyes and quantum dots (QDs), which involves simultaneous absorption of two or more photons through virtual states.[4] The efficiency of a UC process is generally several orders of magnitude higher than that of nonlinear multiphoton absorption, thus enabling UC to be produced by a low-cost continuous-wave (CW) diode laser instead of the need of ultrashort pulse lasers for nonlinear multiphoton excitation. The UCNPs have multiple attributes that make them well-suited for use in theranostics comprised of imaging, drug delivery, and therapy. Their unique frequency conversion capability is usually unavailable for endogenous and exogenous fluorophores, thus providing UCNPs numerous distinctive characteristics for medical diagnostics and therapy.

Dynamics and Fluctuations in Biomedical Photonics XIV, edited by Valery V. Tuchin, Kirill V. Larin,
Martin J. Leahy, Ruikang K. Wang, Proc. of SPIE Vol. 10063, 100631A · © 2017 SPIE
CCC code: 1605-7422/17/$18 · doi: 10.1117/12.2250587

For imaging, some of the advantages are: 1) virtually zero autofluorescence background allowing one to improve signal-to-noise ratio; 2) large anti-Stokes shifts allowing one to separate easily the photoluminescence from the excitation wavelength; 3) narrow emission bandwidths allowing for multiplexed imaging; and 4) high resistance to photobleaching making it suitable for long-term repetitive imaging. In addition, UCNPs are nonblinking, less light scattering, and allow for deep tissue probing because of excitation being in the NIR region that is within the optical transparency window. Moreover, a new direction for theranostic UCNPs, utilizes hierarchically built nanostructures to combine UC photoluminescence (PL) imaging with other imaging modalities such as magnetic resonance imaging (MRI),[5] computed tomography (CT),[6] single-photon emission computed tomography (SPECT),[7] positron emission tomography (PET),[8] as well as with therapeutics such as photothermal therapy (PTT),[9] photodynamic therapy (PDT),[10,11] and gene and drug delivery.[12] Indeed, significant advances in theranostics at application of UCNPs have been recently made by use of nanochemistry that allows one to control their optical properties aiming to enhance upconversion at a selected wavelength,[13] surface modification for phase transfer,[14] and surface coupling chemistry for ligands that are targeting biomarkers.[15] The UCNPs have been extensively used for studies on imaging of living tissues and phantoms,[16,17] and are also quite promising for temperature sensing.[18,19]

Adipose tissue surrounding the tumor and it is therefore important to remove it to ensure optical access to the tumor. There are novel least-invasive optical methods providing reduction of regional or site-specific accumulations of abdominal fat (so-called belly fat or stomach fat) under development. Structural alterations of the adipose tissue also take place due to temperature change.[20] A heating of the adipose tissue (AT) above the normal physiological range (~43-44 °C) causes degradation of fat cells[21] affecting tissue optical properties. The higher orders of unsaturated fatty acids have lower melting points.[22] In clinical practice, an insufficient heating during treatment does not result in a required therapeutic effect, whereas the overheating leads to the damage of healthy tissues. Therefore, arranging optimal irradiation conditions is a crucial task for development of the laser photothermal therapy. The direct measurement of thermal fields in the adipose tissue in proximity to thermophotosensitizers is an attractive feature for monitoring and subsequent control of the tissue heating. At the same time, the photothermal treatment efficiency depends on the AT state because of the heating process is associated with the phase transitions. The AT is characterized by a relatively low melting temperature range, close to the physiological conditions.[23] Several phase transitions take place within 24…45 ºC.[24-26]

One of the potentially promising methods for monitoring of the local temperature in tissue is based on the luminescence of nanoparticles embedded into a heated region.[27,28] Due to reduction of scattering of the heated AT that is similar to optical clearing, an alteration in the luminescent intensity occurs.[29]

The major goal of the present study is the application the thermosensitive luminescent UCNPs ($NaYF_4$:Yb^{3+}, Er^{3+}) for temperature monitoring within adipose tissues *in vitro* in a wide temperature range, from room to human body and further to hyperthermic temperatures. Two types of UCNP specimens, namely, synthesized powdered as-is and embedded into polymer film were used.

2. EXPERIMENTAL PROCEDURES

In this study, made in-house upconversion nanoparticles of sodium yttrium fluoride co-doped with Er^{3+} and Yb^{3+} ions ($NaYF_4$:Yb^{3+}, Er^{3+}) were used. The nanoparticles (ca. 220 nm in size, see Figure 1) were synthesized by a hydrothermal method. Field emission scanning electron microscope (MIRA 2 LMU, TESCAN) was used to obtain images of particles. The particles were coated with SiO_2 (powder), or placed into a cellulose acetate film. Recently, low cytotoxicity of such nanoparticles was shown.[31]

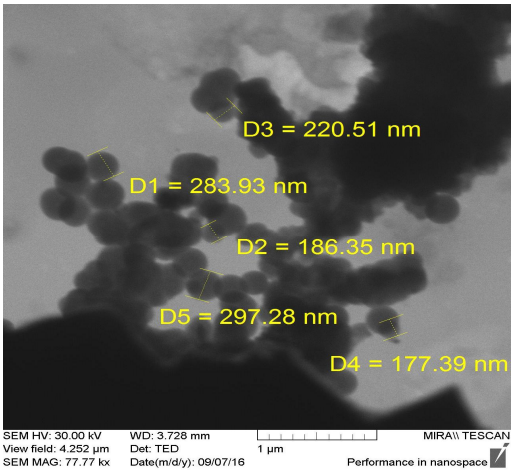

Figure 1. SEM (MIRA 2 LMU, TESCAN) image of the [$NaYF_4$: Er^{3+}, Yb^{3+}] UCNPs.

Figure 2 shows a schematic diagram of the experimental setup for the measurement of the temperature dependence of the UCNP luminescence intensity. The particles were heated using a Peltier element with a temperature control sensor (Perkin Elmer PTP 1, USA). Heating temperature was varied from 25 °C to 70 °C with increment of 5 °C. The samples were kept at each temperature for 5 min. UCNP luminescence was excited by a laser diode with the wavelength of 980 nm, output power 108 mW and laser spot size 2.3×3 mm^2 (DMH980-200, B&W Grason Technology CO., Ltd., China). The luminescence spectra of the nanoparticles were recorded using a spectrometer (Ocean Optics QE6500 FL, USA). The spectra were measured at a 500-ms integration time. A colored-glass light filter SZS-21 was used to suppress the scattered excitation light. IR imager IRISYS 4010 (InfraRed Integrated System Ltd, UK) located at a distance of 30 cm from a sample was used for non-contact measurement of a surface temperature of samples.

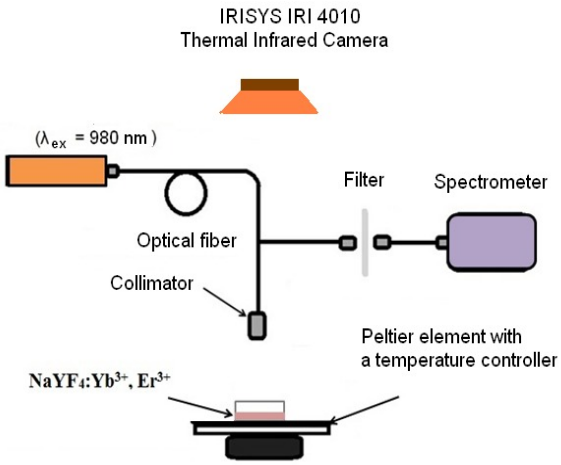

Figure 2. Experimental setup for the measurement of the temperature dependence of the luminescence intensities of UCNPs ($NaYF_4$:Yb^{3+}, Er^{3+})

Samples of human abdominal adipose tissue (AT) taken after plastic surgery have been studied. The experimental study was conducted in the Centre of Collective Use of Saratov State Medical University (Russia). After freezing at temperature -18°C for 10 hrs, the samples were cut into thin slices (0.1 - 0.4 mm thick). Thickness of the samples was measured with a micrometer at several points in the sample sandwiched between two cover glasses. The thickness was averaged by 5 points with the typical SD of 0.02 mm. The AT samples under study were placed on a black surface of the heating element above nanoparticles.

Optical properties of the adipose tissue were determined using a spectrophotometer (Shimadzu UV-3600, Japan) with an integrating sphere in the spectral range of 300–2500 nm. The area of the samples was 3.0 - 3.4 cm^2. The thickness of experimental samples varied, amounting on average to 0.30±0.03 mm before exposure and 0.13±0.03 mm thereafter. To monitor all of adipose tissue phase transitions, temperature was varied from 25°C to 70°C with increment of 5°C. To heat the samples, a thermoresistor controled by applied voltage was used.

3. EXPERIMENTAL RESULTS AND DISCUSSION

The luminescence spectra of the UCNPs ($NaYF_4$:Yb^{3+}, Er^{3+}) for different temperatures: the film with the particles and the powder are shown in Figure 3.

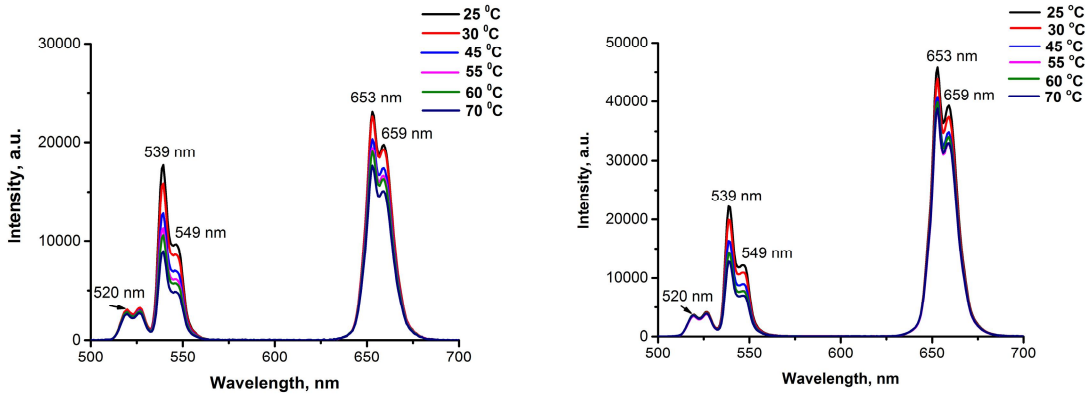

Figure 3. The luminescence spectra of the UCNPs for different temperatures: the film with the particles (a) and the powder (b); λ_{ex} = 980 nm.

The energy transfer from the Yb^{3+} ion to the Er^{3+} ion results in the transition of the acceptor to the $^4F_{7/2}$ level followed by nonradiative relaxation to the $^4S_{3/2}$ level (Figure 4). The $^2H_{11/2}$ level can also be populated, as it is in thermal equilibrium with the $^4S_{3/2}$ level. The populations of these closely spaced levels are described by the Boltzmann distribution law. The Er^{3+} ion can decay radiatively to the ground state from the $^4S_{3/2}$ and $^2H_{11/2}$ levels, emitting green light of wavelengths around 550 and 525 nm, respectively. Each band is composed of numerous narrow emission peaks that are caused by Stark splitting. Because the luminescence intensity is proportional to the population of the excited level, the intensity ratio is described also by the Boltzmann law:

$$I_1(\lambda_1)/I_2(\lambda_2) = C \exp(-\Delta E/k_B T), \quad (1)$$

where $I_1(\lambda_1)$ and $I_2(\lambda_2)$ are the emission intensities of the $^4S_{3/2} \rightarrow {}^4I_{15/2}$ and $^2H_{11/2} \rightarrow {}^4I_{15/2}$ transitions of the Er^{3+} ion, respectively (in our experiments, λ_1 = 546 nm and λ_2 = 520 nm); C is a normalization factor (C is a constant) dependent on the degree of degeneracy of energy level, the rate of spontaneous emission, and the energy of emitted photon; ΔE is the energy gap between the two excited levels, given by $\Delta E = h\Delta\nu$, where h is the Planck's constant, k_B is the Boltzmann's constant, and T is the absolute temperature. According to Ref. [30], to measure the local temperature of the UCNPs, the values of the natural logarithm of the ratio of the nanoparticle luminescence intensities at the wavelengths λ_1 = 546 nm and λ_2 = 520 nm were calculated. The temperature dependence is approximated as

$$\mathrm{Ln}(I_1/I_2) = \mathrm{Ln}C + \Delta E/k_B T = A + B \times T, \quad (2)$$

The accuracy of temperature measurement should be determined by the energy-gap parameter. Figure 5 shows the obtained logarithmic temperature dependences for the ratio of luminescence intensities at the wavelengths λ_1 = 546 nm and λ_2 = 520 nm of the UCNP ($NaYF_4$:Yb^{3+}, Er^{3+}) polymer film (Figure 5a) and powder (Figure 5b) and for the same UCNP samples, covered with a layer of AT with the thickness 0.1 and 0.2 mm, respectively.

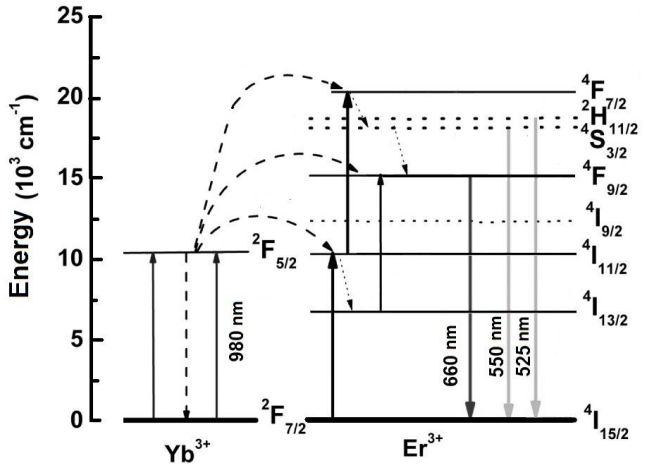

Figure 4. Schematic representation of the energy levels in the system of the Yb^{3+} and Er^3 ions.

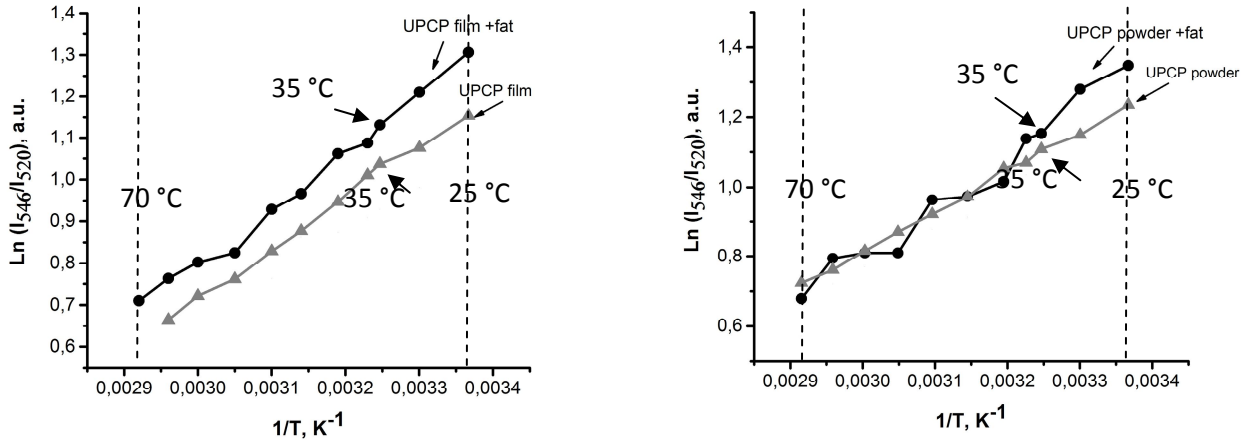

a) b)

Figure 5. Temperature dependences of the natural logarithm of the ratio of luminescence intensities at the wavelengths λ_1 = 546 nm and λ_2 = 520 nm of the UCNP ($NaYF_4$:Yb^{3+}, Er^{3+}) polymer film (a) and powder (b) and for the same UCNP samples (+fat), covered with a layer of AT with the thickness 0.1 and 0.2 mm, respectively

The values of slope angles of the approximating lines for the UCNP polymer film and the UCNP powder obtained from the energy difference between the two excited levels of erbium are presented in Table 1.

Table 1. Results of fitting for powder and film UCNPs

	Film Ln ($I_{\lambda546}$/ $I_{\lambda520}$)	Powder Ln ($I_{\lambda546}$/ $I_{\lambda520}$)	Calculation, Eq. (2)
A	-2.78	-2.63	
B	1230.2	1148.5	990.0

Referring to Figure 5, the coincidence of the temperature dependences of the natural logarithm of the ratio of luminescence intensities at the wavelengths λ_1 = 546 nm and λ_2 = 520 nm between the polymer film with the UCNPs and the same film covered with a layer of AT is worse than that for the UCNP powder.

Optical parameters of biological tissue in one phase state are constant; during phase transition, they change, in particular, refractive index discontinuously.[32] The increase of luminescence intensity at high temperatures can be explained by tissue clearing associated with the phase transition of lipids. This is evident, for example, from the temperature dependence of the luminescence intensity of the $NaYF_4$:Yb^{3+}, Er^{3+} nanoparticles presented in Figure 6.

After the first phase transition (35 - 40°C) in AT, the temperature dependences for the powder and the powder covered with adipose tissue are almost identical. The small difference can be explained by a good contact of UCNPs with AT. For the film, the dependence is shifted up by a substantial constant value. In logarithmic dependence, this corresponds to the appearance of a factor in the luminescence intensity ratio. This factor can be due to difference of losses arising from scattering for two different wavelengths 546 and 520 nm and the absence of direct contact of UCNPs in polymer film with AT.

The intensity ratio of the luminescence transmitted through the AT layer and obtained directly from the sample with the nanoparticles should characterize changes in scattering properties of adipose tissue under changes of temperature. Since scattering decreases with increasing wavelength, we have considered the following dependence for two wavelengths 539 and 653 nm. As Figure 6 suggests, at the wavelengths of λ_1 = 539 nm and λ_2 = 653 nm, the AT phase transition at a temperature of 55°C is more pronounced for the films with the nanoparticles than for the powder.

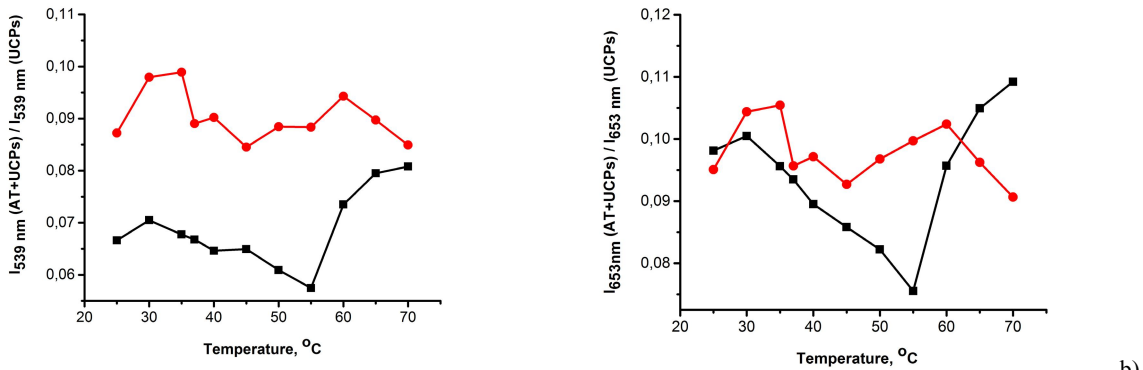

a) b)

Figure 6. Temperature dependence of the ratio of luminescence intensities at 539 nm (a) and 653 нм (b) for UCNP samples with AT layer and without: film (■) and powder (●), AT layer thickness 0.1 and 0.2 mm, respectively.

Scattering changes during phase transitions are also observed directly in the temperature dependences of the luminescence intensity (Figure 7). In the figure, the curves obtained for luminescence and collimated transmission of AT samples (T_c) were combined. Behavior of the collimated transmittance changes abruptly in the region of 55 - 60°C. The luminescence intensity changes synchronously. At the same time, the phase transition in the region of 30-35°C is sufficiently clear to be seen on the luminescence curves. It should be noted that AT clearing through heating is better observed for the sample with the UCNP film.

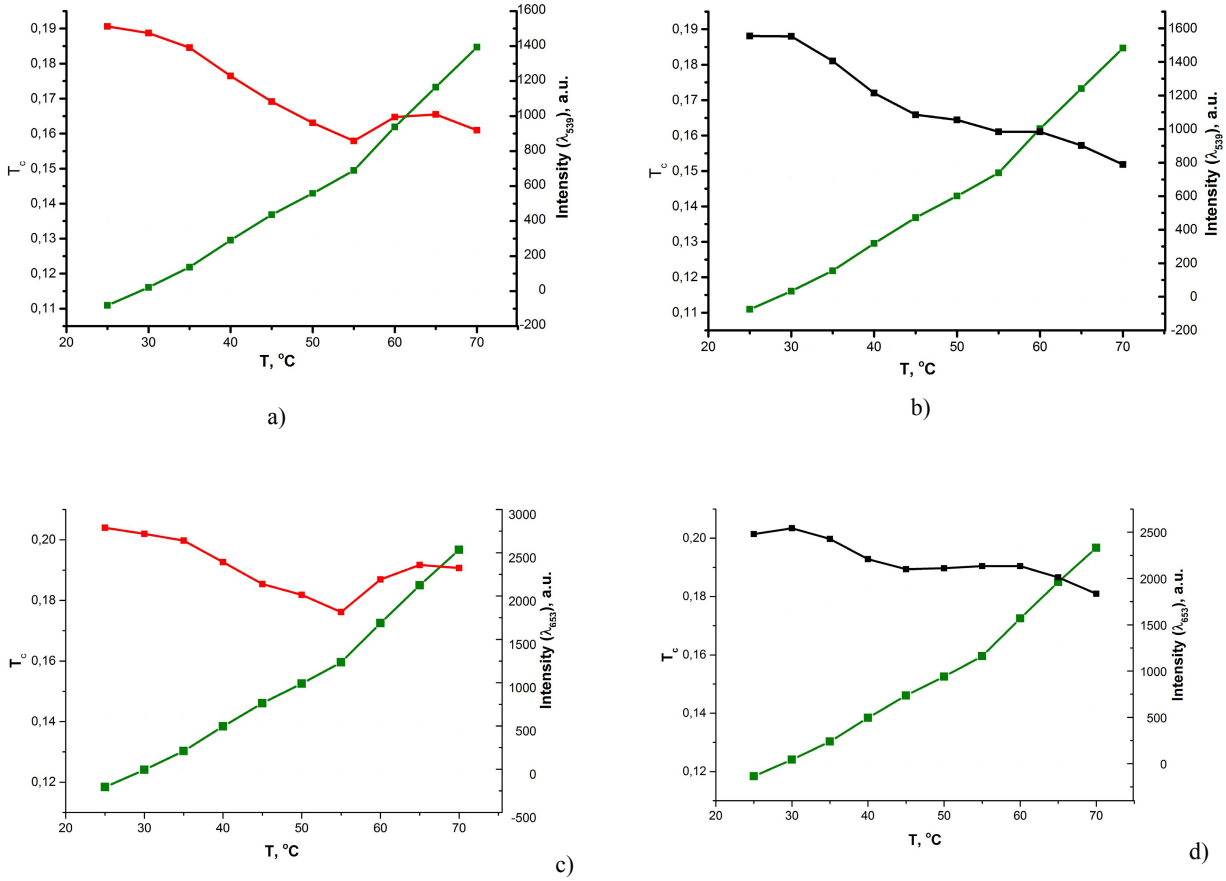

Figure 7. Temperature dependences of the collimated transmittance T_c of AT sample (0.33 mm) (green); UCNP luminescence intensity at 539 nm and 653 nm for film (a and c) (red) and powder (b and d) (black), AT layer of thickness 0.1 and 0.2 mm, respectively

4. CONCLUSIONS

It has been shown the possibility of applying of the thermosensitive luminescent UCPs [$NaYF_4$:Yb^{3+}, Er^{3+}] for temperature monitoring in adipose tissues *in vitro* in a wide temperature range, from room to human body temperatures and above. The synthesized powdered UCNPs were used as-is and as embedded into polymer film. Temperature dependences of the UCNP luminescence spectra for the UCNP polymer film and powder have been obtained. Since the temperature detection sensitivity should be determined by the energy-gap parameter, the temperature dependences of the natural logarithm of the ratio of UCNP luminescence intensities at the wavelengths λ_1 = 546 nm and λ_2 = 520 nm for the polymer film and the powder, and for the same nanoparticle samples covered with a layer of adipose tissue were obtained.

The observed coincidence of the temperature dependences of the natural logarithm of the ratio of UCNP luminescence intensities at the wavelengths λ_1 = 546 nm and λ_2 = 520 nm between the UCNP polymer film and the same film covered with a layer of adipose tissue is worse than that for the UCNP powder.

The increase in luminescence intensity at high temperatures can be explained by tissue clearing associated with the phase transition of lipids.

The intensity ratio of the luminescence transmitted through the adipose tissue layer and obtained directly from the sample with the nanoparticles characterize changes in scattering properties of adipose tissue under changes of temperature. The adipose tissue phase transition at a temperature of 55°C is more pronounced for the films with the nanoparticles than for the powder. At the same time, three phase transitions (at the temperatures of 35, 55 and 60°C) can be observed for the powder. The differences in the results can be partly explained by differences in the scattering properties of the samples: luminescence light backscattering by the powdered nanoparticles surrounded by adipose tissue in our experiments is substantially weaker than that by the nanoparticles embedded into polymer film.

The temperature dependences obtained for UCNP luminescence and collimated transmission of an adipose tissue sample demonstrate the ability to detect phase transitions in adipose tissue. Behavior of the both dependencies changes abruptly in the region of 55 - 60°C. At the same time, the phase transition in the region of 30-35°C is sufficiently clear to be seen only on the luminescence curves. It should be noted that adipose tissue clearing through heating is substantially more effective for the UCNP film than for the UCNP powder.

Thus, we can conclude that the possibility of simultaneous registration of the temperature of UCNPs placed under a layer of adipose tissue and the phase transitions of adipocyte lipids was demonstrated.

ACKNOWLEDGMENTS

The authors would like to acknowledge the support from Russian Federation President Grant for state support of young Russian scientists № MK-6009.2016.2 (IYuY and EKV), Russian Presidential grant NSh-7898.2016.2 (IYuY, EKV, VIK, JGK and VVT), the Russian Governmental grant 14.Z50.31.0004 (VVT), The National Research Tomsk State University Academic D.I. Mendeleev Fund Program (IYuY, EKV, VIK, and VVT).

References

[1] Selvan, S. T., Tan, T. T. Y., Yi, D. K., and Jana, N. R. "Functional and multifunctional nanoparticles for bioimaging and biosensing," *Langmuir* **26**, 11631–11641 (2010).
[2] Auzel, F. "Upconversion and anti-stokes processes with f and d ions in solids," *Chem. Rev.* **104**, 139–174 (2004).
[3] Wang, F., and Liu, X., "Recent advances in the chemistry of lanthanide-doped upconversion nanocrystals," *Chem. Soc. Rev.* **38**(4), 976-989 (2009).
[4] He, G.S., Markowicz, P.P., Lin, T.-C., and Prasad, P.N., "Observation of stimulated emission by direct three-photon excitation," *Nature* **415**, 767-770 (2002).
[5] Kumar, R., Nyk, M., Ohulchanskyy, T.Y., Flask, C.A., and Prasad, P.N., "Combined Optical and MR Bioimaging Using Rare Earth Ion Doped $NaYF_4$ Nanocrystals," *Adv. Funct. Mater.* **19**(6), 853-859 (2009).
[6] Xing, H., Bu, W., Zhang, S., Zhen, X., Li, M., Chen, F., He, Q., Zhou, L., Peng, W., Hua, Y., and Shi, J., "Multifunctional nanoprobes for upconversion fluorescence, MR and CT trimodal imaging," Biomaterials 33(4), 1079-1089 (2012).
[7] Yang, Y., Sun, Y., Cao, T., Peng, J., Liu, Y., Wu, Y., Feng, W., Zhang, Y., and Li, F., "Hydrothermal synthesis of NaLuF4:153Sm,Yb,Tm nanoparticles and their application in dual-modality upconversion luminescence and SPECT bioimaging," *Biomaterials* **34**(3), 774-783 (2013).
[8] Sun, Y., Yu, M., Liang, S., Zhang, Y., Li, C., Mou, T., Yang, W., Zhang, X., Li, B., Huang, C., and Li, F., "Fluorine-18 labeled rare-earth nanoparticles for positron emission tomography (PET) imaging of sentinel lymph node," *Biomaterials* **32**(11), 2999-3007 (2011).

[9] Cheng, L., Yang, K., Li, Y., Chen, J., Wang, C., Shao, M., Lee, S.-T., and Liu, Z., "Facile Preparation of Multifunctional Upconversion Nanoprobes for Multimodal Imaging and Dual-Targeted Photothermal Therapy," *Angew. Chem. Int. Ed.* **50**, 7385–7390 (2011).
[10] Wang, F., "Upconversion nanoparticles in biological labeling, imaging, and therapy," *Analyst* **135**, 1839–1854 (2010)
[11] Idris, N.M., Gnanasammandhan, M.K., Zhang, J., Ho, P.C., Mahendran, R., and Zhang, Y., "In vivo photodynamic therapy using upconversion nanoparticles as remote-controlled nanotransducers," *Nat. Med.* **18**, 1580–1585 (2012).
[12] Wang, C., Cheng, L., and Liu, Z. "Drug delivery with upconversion nanoparticles for multi-functional targeted cancer cell imaging and therapy," *Biomaterials* **32**(4), 1110-1120 (2011).
[13] Chen, G., Ohulchanskyy, T.Y., Kumar, R., Ågren, H., and Prasad, P.N., "Ultrasmall Monodisperse NaYF4:Yb3+/Tm3+ Nanocrystals with Enhanced Near-Infrared to Near-Infrared Upconversion Photoluminescence," *ACS Nano* **4**(6), 3163–3168 (2010).
[14] Bogdan, N., Vetrone, F., Ozin, G.A., and Capobianco, J.A., "Synthesis of Ligand-Free Colloidally Stable Water Dispersible Brightly Luminescent Lanthanide-Doped Upconverting Nanoparticles," *Nano Lett.* **11**(2), 835–840 (2011).
[15] Chen, Z., Chen, H., Hu, H., Yu, M., Li, F., Zhang, Q., Zhou, Z., Yi, T., and Huang, C., "Versatile Synthesis Strategy for Carboxylic Acid−functionalized Upconverting Nanophosphors as Biological Labels," *J. Am. Chem. Soc.* **130**(10), 3023–3029 (2008).
[16] Grebenik, E.A., Nadort, A., Generalova, A.N., Nechaev, A.V., Sreenivasan, V.K., Khaydukov, E.V., Semchishen, V.A., Popov, A.P., Sokolov, V.I., Akhmanov, A.S., Zubov, V.P., Klinov, D.V., Panchenko, V.Y., Deyev, S.M., and Zvyagin, A.V., "Feasibility study of the optical imaging of a breast cancer lesion labeled with upconversion nanoparticle biocomplexes," *J. Biomed. Opt*. **18**(7), 076004 (2013).
[17] Khaydukov, E.V., Zhu, X., Lu, Y., Zhao, J., Feng, W., Jia, G., Wang, F., Li, F., and Jin, D., "High-contrast fibre-optic visualization of upconverting nanoparticle labels in scattering media," *Laser. Phys. Lett.* **11**(9), 095602 (2014).
[18] Wang, X., Zheng, J., Xuan, Y., and Yan, X., "Optical temperature sensing of NaYbF4: Tm3+ @ SiO2 core-shell micro-particles induced by infrared excitation," *Opt. Express* **21**(18), 21596-21606. (2013)
[19] Hao, S., Chen, G., and Yang, C., "Sensing Using Rare-Earth-Doped Upconversion Nanoparticles," *Theranostics* **3**(5), 331–345 (2013).
[20] Belikov, A.V., Prikhod'ko, K.V., and Smolyanskaya, O.A., "Study of thermo induced changes resulted in optical properties of fat tissue," *Proc. SPIE* **5066**, 207-212 (2003).
[21] Salzman, M.J., "Laser lipolysis using a 1064/1319-nm blended wavelength laser and internal temperature monitoring," *Semin. Cutan. Med. Surg*. **28**(4), 220-225 (2009).
[22] S. Ojha, H. Budge, M.E. Symonds, "Adipocytes in Normal Tissue Biology," in *Pathobiology of Human Disease. A Dynamic Encyclopedia of Disease Mechanisms*, *Part II: Organ Systems Pathophysiology,* L. M. McManus, R. N. Mitchell, Eds., pp. 2003-2013, USA, Elsevier, Medical, ACADEMIC PRESS (2014).
[23] Hrdinka, C., Zollitsch, W., Knaus, W., Lettner, F., "Effects of dietary fatty acid pattern on melting point and composition of adipose tissues and intramuscular fat of broiler carcasses" *Poult. Sci.* **75**, 208-215 (1996).
[24] Turk, S.N., and Smith, S.B., "Carcass fatty acid mapping," *Meat. Sci.* **81**, 658-663 (2009).
[25] Schmidt-Nielsen, S., "Melting points of human fats as related to their location in the body," *Acta. Physiol. Scand.* **12**(2-3), 123-129 (1946).
[26] Beadle, B.W., Wilder, O.H.M., and Kraybill, H.R. "The deposition of trienoic fatty acids in the fats of the pig and the rat," *J. Biol. Chem*. **175**, 221-229 (1948).
[27] Yanina, I. u., Volkova, E.K., Popov, A.P., Bykov, A.V., Kochubey, V.I., Skaptsov, A.A., Konyukhova, J.G., Tuchin, V.V. ,"Temperature dependence of the fluorescence spectrum of ZnCdS nanoparticles introduced into adipose tissue *in vitro*," *Proc. SPIE* **9537**, 953724 (2015).
[28] Volkova, E.K., Kochubey, V. I., Konyukhova, J.G., Skaptsov, A.A., Galushka, V., German, S., "Temperature dependence of the fluorescence spectrum of ZnCdS nanoparticles," *Proc. SPIE* **8571**, 85712P (2013).
[29] Popov, A.P., Khaydukov, E.V., Bykov, A.V., Semchishen, V.A., Tuchin, V.V. "Enhancement of upconversion deep-tissue imaging using optical clearing," *Proc. SPIE* **9540**, 95400B (2015).
[30] Vetrone, F., Naccache, R., Zamarrón, A., Juarranz de la Fuente, A., Sanz-Rodríguez, F., Martinez Maestro, L., Martín Rodriguez, E., Jaque, D., García Solé, J., Capobianco, J.A. "Temperature Sensing Using Fluorescent Nanothermometers", *ACS NANO* **4**(6), 3254-3258 (2010).

[31] Guller A.E., Generalova A.N., Petersen E.V., Nechaev A.V., Trusova I.A., Landyshev N.N., Nadort A., Grebenik E.A., Deyev S.M., Shekhter A.B., Zvyagin A.V. "Cytotoxicity and non-specific cellular uptake of bare and surface-modified upconversion nanoparticles in human skin cells," *Nano Research* **8**(5), 1546-1562 (2015).
[32] Haruna, M., Yoden, K., Ohmi, M., and Seiama, A., "Detection of phase transition of a biological membrane by precise refractive-index measurement based on the low coherence interferometry," *Proc. SPIE* **3915**, 188-193 (2000).